Adsorption (2013) 19:979–987
DOI 10.1007/s10450-013-9512-9

Methane adsorption and diffusion in a model nanoporous carbon: an atomistic simulation study

Saeid Yeganegi · Fatemeh Gholampour

Received: 29 July 2012 / Accepted: 8 February 2013 / Published online: 20 February 2013

Abstract A constricted slit model was introduced to improve, one step further, the performance of the simple slit model in prediction of the adsorption and diffusion behavior of simple molecules in the nanoporous carbons (NPCs). The grand canonical Monte Carlo (GCMC) and molecular dynamics (MD) simulations are performed to study the adsorption and diffusion behavior of methane within the constricted slit models. The models are called slit-1, 2, and 3 with constriction heights 5, 7, and 9 Å respectively. For comparison, we used the slit-0 name for the simple slit without constriction. Adsorption results show that at low pressures, the constriction increases the adsorbed amount irrespective of its height. Slit-2 with a constriction height as a molecular diameter has the greatest heat of adsorption and has highest loading at pressures up to 3,000 kPa. At high pressures, when all pores are filled, the adsorption trend is in line with the pore volumes of slits where slit-0 with higher pore volume is dominant. The density profiles in the models were calculated and examined. The spatial distribution of adsorbed methane molecules was examined by various radial distribution functions calculated by MD. Also, MD simulation results show that the diffusion coefficient of methane decreases in constricted slits. The calculated diffusion coefficients in slit-2 in the direction of the constriction are one order of magnitude smaller than the calculated one in the simple slit model but it is far from the experimental values in the NPCs.

S. Yeganegi (✉) · F. Gholampour
Department of Physical Chemistry, Faculty of Chemistry, University of Mazandaran, Babolsar, Iran
e-mail: yganegi@umz.ac.ir

Keywords Constricted slit · Molecular simulation · Adsorption · Diffusion

1 Introduction

The usage of nanoporous carbons (NPCs) in gas separation technologies, especially in natural gas treatment is widely investigated by researchers because of their large porous volumes, high surface area, low production cost, etc. (Golebiowska et al. 2012; Esteves et al. 2008; Wang et al. 2011; Lucenaa et al. 2010). Because of the nanoscopic nature of adsorption and diffusion mechanisms in the NPCs, atomistic simulations are needed for studying these phenomena. The main problem in simulating the NPCs is modeling their amorphous structure (Palmer et al. 2011; Firouzi and Wilcox 2012; Arora and Sandler 2007; Peng and Morris 2010).

Very recently Palmer and Gubbins (2012) reviewed the atomistic models for disordered nanoporous carbon. According to Palmer and Gubbins (2012), there are two major approaches to model the nanostructure of NPCs. The most widely used approach is to construct models from a pre-defined set of elementary building blocks such as aromatic rings and graphene fragments. These models have been successful in capturing many aspects of real NPCs, including variable pore size and pore connectivity. But the predictive capabilities of these models are limited since they assume significant prior knowledge of the carbon chemistry and nanostructure. There are no rigorous guidelines based on physical principles to suggest how these building blocks should be defined or pieced together. The other approach, build structural models from the ground up, predicting the nanostructure and porous features of NPCs use techniques that are rooted in statistical

mechanics. In these methods explicitly treat the chemical bonding between carbon atoms in order to predict the formation of the various structural features that are found in real NPCs. Their predictive capability depends on the method that dynamically describes the formation and disassociation of chemical bonds between carbon atoms during the simulations. Using of the first principle methods for describing bond formation and disassociation is limited to the small systems. Alternatively, classical reactive force fields can be used for simulation of larger systems which are generally required to capture many of the structural and porous features found in NPCs. Unfortunately; both of these approaches are computationally intensive. Furthermore, for the classical reactive force field approach, the predictive ability depends heavily on the quality of the force field and simulation conditions.

Slit model of graphite is the simplest model for simulating NPCs (Striolo et al. 2003; Severson and Snurr 2007; Sitprasert et al. 2011; López et al. 2011; Palmer and Gubbins 2012; Billemont et al. 2011; Heuchel et al. 1999). This model has good results in predicting adsorptive behavior of more ordered carbon materials such as carbon blacks, but not successful in representing structure related and diffusive properties of NPCs (Palmer and Gubbins 2012). In addition to several simulation studies carried out on the adsorption of gases on the slit model (Striolo et al. 2003; Severson and Snurr 2007; Sitprasert et al. 2011; López et al. 2011; Palmer and Gubbins 2012; Billemont et al. 2011; Heuchel et al. 1999), recently, permeability of methane across carbon slit pores were investigated by Lim and Bhatia (2011). They simulated adsorption and diffusion of the united atom model of methane for the several pore width of the carbon slit model. They compared the resulted permeabilities with the experimental values for some porous carbons, and showed that their simulated permeabilities are much larger than the experimental results. They argued that it is necessary to take into account the pore mouth resistance, and the pore connectivity and morphology to predict the macroscopic permeability by simulation.

Detailed modeling of the NPCs requires a complete understanding of the relationship between their nanostructure and functional properties. Achieving this level of understanding for NPCs is extremely challenging because of their heterogeneity, pore size variation and morphology. The adsorption phenomena are modified by the change in the potential field. There are a number ways in which the potential field can be changed. The field can be changed by introducing defects, surface roughness, or heterogeneities along the length of a single pore. Jagiello and Olivier (2009) proposed a model of slit pores having parallel circular walls "cut" from graphene sheets as a step toward a model of independent finite slit pores instead of the standard infinite slit pore model. They concluded that introducing one additional variable describing the carbon pore wall diameter improves the description of the NPC structure. Phuong (2011) studied argon adsorption in connected cylindrical pores with different sizes. They have explored the effect of the neck and cavity length on the cavitation and pore blocking. Also Fan et al. (2011) studied the argon adsorption in various models including ink-bottle pore and cavity connected to smaller necks.

In this study we approximated the NPCs by a constricted slit pore model. The details of the model will be explained in the simulation details section. We proposed this simple model to introduce the effect of the variation of the pore width in NPCs on the gas permeability in the simplest way as possible. Also, the other difference of our study is that our methane model is five sites, rather than one-site methane model that used by Lim and Bhatia (2011). In what follows, we first explain the constricted slit models and details of simulations and then the results of the adsorption isotherm and diffusion coefficient calculations using grand canonical Monte Carlo (GCMC) and Molecular dynamics (MD) simulations.

2 Simulation details

As depicted in Fig. 1 two slit types have been used in this work. A simple flat slit was constructed from ideal graphene sheets, periodic in the x–y-plane, with unit cell dimensions of 30.7, 72 and 80 Å along the x, y and z-axis, respectively. The pore width in the z direction was set to 20 Å then the distance between each unit cell in the z direction was 30 Å. This spacing between the unit cells in the z direction was used to prevent the artifact interaction between the gas molecules in the adjacent unit cells (Nasrabadi and Foroutan 2012; Ho et al. 2012; Foroutan and Nasrabadi 2011). To construct the constricted models the graphite sheets were limbered in 5 points in the y direction. The height and length of the constriction in the constricted part were set at 5, 7, 9 and 11.2 Å. Figure 1 shows the simple and constricted slit models. As shown in Fig. 1, the numbers 0, 1, 2 and 3 are used for simple and constricted slits with 5, 7, 9 constriction heights respectively.

Grand canonical Monte Carlo simulations are performed for studying adsorption of methane. In GCMC simulation, the chemical potential, volume and the temperature of the simulation box are kept constant and fluctuations in the number of adsorbate molecules, pressure and the energy are allowed (Allen and Tildesley 1987). In fact the fugacity of adsorbate gas in a hypothetical bulk phase that is in equilibrium with the adsorbed gas in the simulating box should be set. So an equation of state should be used to relate the fugacity of the gas to the pressure of the system.

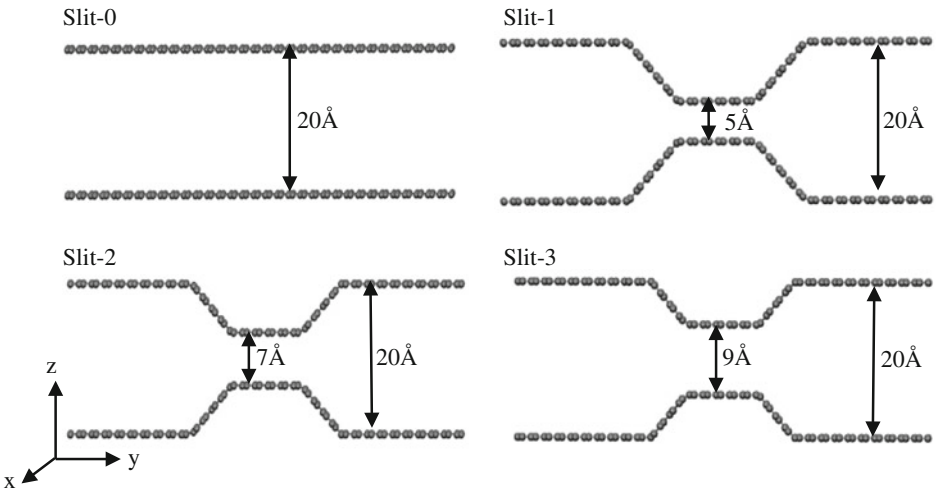

Fig. 1 The studied slit models: slit-0 without constriction, slits-1, 2, and 3 with constriction heights: 5, 7, and 9 respectively

Each pore wall was modeled as a sheet of graphene. The carbon atoms in the graphene sheets were modeled as Lennard-Jones particles (Palmer et al. 2011) corresponding to sp^2 carbon atoms, where their potential parameters are shown in Table 1; the positions of these carbon atoms are kept fixed throughout our simulations. The methane molecules were modeled using an all atom model (Anderson et al. 2011). In this model the C–H bond length is 1.09 Å and the H–C–H angle is 109.5. The potential parameters and atomic charges used for methane are also listed in Table 1. The cross LJ parameters are obtained using the Lorentz–Berthelot mixing rules (Allen and Tildesley 1987). The cutoff distance for calculating LJ interactions was 15 Å.

We used the Peng–Robinson equation of state (Ahmad et al. 2008) for relating the input pressure to the fugacity of CH_4. The adsorbent–adsorbate interactions were summed over all pairs of slit carbon atoms and CH_4 interaction sites. The columbic interactions were calculated using the Ewald summation method. Periodic boundary conditions were applied in all three dimensions. The simulations carried out at the temperature of 298.15 K and pressures from 1 to 10,000 kPa.

The grand canonical Monte Carlo simulations were used for studying adsorptive behavior of methane in slits. For each GCMC simulation 2×10^7 moves were attempted. The first 5×10^6 moves were used for equilibration and the remaining 1.5×10^7 moves for computing the ensemble averages. Four types of trial moves were randomly attempted in the GCMC simulations: displacement, rotation, and swap with reservoir including creation and deletion with equal probability. For reporting the loadings, we averaged the number of adsorbed CH_4 molecules in the interior of slit over the production step.

Table 1 Potential model parameters used in simulations

Atom	σ (Å)	ε/k_B (K)	q(e)	Reference
C (slit)	3.4	28	–	Palmer et al. (2011)
C (CH_4)	3.40	55.055	−0.660	Anderson et al. (2011)
H (CH_4)	2.65	7.901	+0.165	

The Molecular dynamics simulations were used for examining the dynamic behavior of adsorbed methane within the constricted slits. We used the DL-POLY package (Smith et al. 2009) for MD simulations. The initial configuration for each MD simulation was the equilibrated configuration of the corresponding GCMC simulation. A time step of 1 fs was used for integrating the equations of motion. The MD simulations are carried out in an NVT ensemble with Nose–Hoover thermostat where the relaxation time used for the thermostat was 0.1 ps. The MD simulations were conducted for 2×10^6 time steps and the last 1.4×10^6 steps were used for collecting the ensemble averages.

3 Results and discussion

3.1 GCMC results

The calculated adsorption isotherms from the GCMC simulations at 298.15 K of temperature and pressures up to 10,000 kPa are plotted in Fig. 2. As shown in Fig. 2, at pressures lower than 3,000 kPa the loading in slit-2 was larger than that of the other models… From Fig. 2, one can say that at low pressures, introducing a constriction larger than the size of a methane molecule in the slit model of nanoporous carbon generally increases the adsorption of methane. In the constriction region, because of the vicinity of two slit walls, the adsorbate molecule adsorbs with either top and bottom walls, whereas in slit-0, the distance

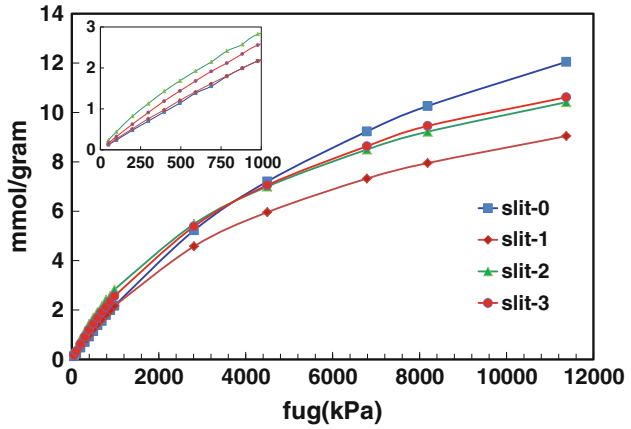

Fig. 2 Adsorption isotherms of CH_4 within the four slit models. The intake depicates the low pressure adsorption isotherms

between two slit walls is larger than 2.5 times of the collision diameter of a greatest adsorbing atom (carbon atom of methane); so the molecules which are attracted to the one side wall, cannot be adsorbed by the opposite wall.

The adsorption trend in slit models becomes different at larger pressures. When the constriction area saturated with adsorbed molecules, the determinant parameter will be the total accessible volume. So, at pressures larger than 3,000 kPa, the adsorption trend follows the pore volumes: slit-0 > slit-3 > slit-2 > slit-1.

Coasne et al. (2006a, b, 2011) studied the adsorption, structure and dynamics of fluids in ordered and disorder carbon models. They find that the filling pressure for a graphite slit pore is well defined and is lower than those for the disordered porous carbon and also the filling of the disordered carbon is continuous and spans over a large pressure range. However, they concluded that the agreement between two models can be improved if the same density of carbon atoms is used. The isotherms in Fig. 2 are similar and do not show the differences between the adsorption isotherms of ordered and disordered carbon porous reported by Coasne et al. (2006a, b, 2011). The constricted slit model does not produce the adsorption behavior much different from the simple slit.

Better explanation of the observed results could be achieved using the snapshots taken from GCMC simulations. Figure 3 illustrates the snapshots taken from the final configurations of simulations at 1,000 and 10,000 kPa of pressures.

At 1,000 kPa the snapshots show that in slit-0 there are well defined methane layers next to the pore walls that adsorbed by the walls, but the second layer is not well formed in the middle of slit height. For slit-1, due to the small size of the pore height in the constriction region, none of CH_4 molecules can be entered into this region. Also the considerable aggregation of molecules at two entrance mouths of this region is explicitly observable. The observed aggregation can be understood in terms of the adsorption of methane molecule by the closing walls of the constriction mouth. In slit-2, a pronounced layer of adsorbed CH_4 molecules are consecutively formed in the constricted region, but in slit-3 the adsorbed molecules are spanning between two walls of constricted region. It is interesting that for the slit-2 there are a large number of the methane molecules near the entrance of the constriction. Snapshots at 10,000 kPa (Fig. 3b) show that at higher pressure the constriction area fills up with adsorbed molecules while there are void spaces and clusters of methane molecules in the flat regions.

To compare our results with experimental results of Anderson and coworkers on NPCs (Anderson et al. 2011), we calculated the equilibrium adsorption isotherm at one of the thermodynamic states of their work. We have chosen the temperature of 100 °C (373.15 K) and pressure of 1,200 kPa. Table 2 represents our calculated loading amounts of methane in the four slit models and the corresponding experimental value of Anderson for NPC.

As in Table 2, our results are in good agreement with experimental results for NPCs. The relatively greater values of loading in slit models can be explained in terms of the complexity of real porous carbon structures with respect to the simple slit models and existence of spaces in their structure that are not actually accessible for adsorbate molecules.

Lim and Bhatia (2011), using a one-site spherical CH_4 molecular model, predicted the methane adsorption isotherms in carbon slit pores of width 6.5–7.5 Å. Their GCMC calculated loadings in the pressure range of 1–1,000 kPa and $T = 298$ K are generally up to 12 mmol/cm^3. Changing the units of our loadings to mmol/cm^3, were the volume in denominator is the accessible pore volume, the calculated loading values for slit-0 at the same condition (lower than 1,000 kPa) will be lower than 3.5 mmol/cm^3. The difference between our values for simple flat slit and that of Lim can be expressed in terms of: 1- in Lim's work, the pore width was only between 6.5 and 7.5 Å, and same as mentioned ago, the adsorbate molecules in this condition are attracting from two slit walls, whereas in our models this could be happening only in constriction regions. 2- Lim modeled CH_4 molecules as neutral spherical LJ sites, whereas we considered an all atom model for CH_4 with partial charges on each LJ site. A neutral methane model enhances the adsorption, whereas partial negative charges on hydrogen atoms, which surrounded the carbon atom, results in an electrostatic repulsion which in turn can lower the adsorption of a methane molecule by an adsorbed one in the adjacent adsorption site.

We have used the direct relation:

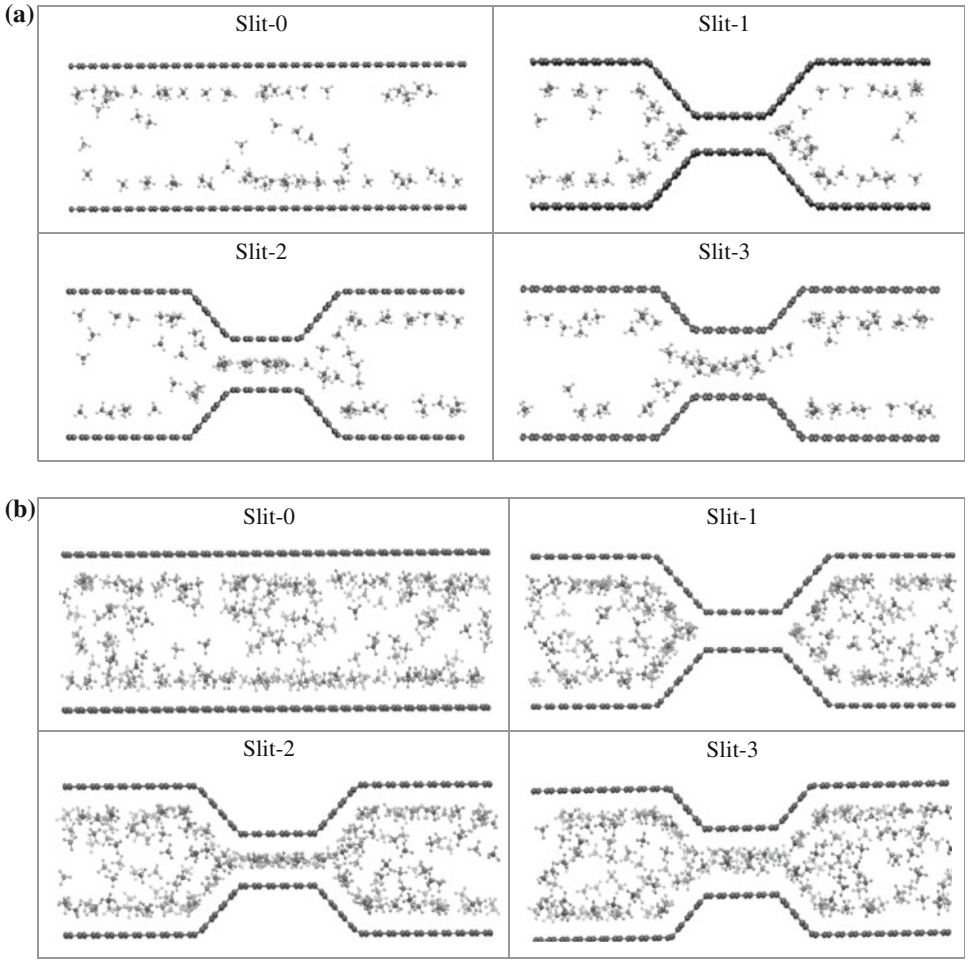

Fig. 3 Snapshots of the final configuration of GCMC simulations at **a** 1,000 kPa and **b** 10,000 kPa

Table 2 Comparison of adsorbed amounts between this study with real NPC result at 373.15 K and 1,200 kPa (Anderson et al. 2011)

	Slit-0	Slit-1	Slit-2	Slit-3	NPC (experiment)
Loading (mmol/g)	1.2311	1.1346	1.4676	1.3790	~0.9

$$q_{\mathrm{st}} = RT - \left(\frac{\partial U}{\partial N_{\mathrm{ad}}}\right)_{T,V} \quad (1)$$

for estimating the isosteric heat of adsorption (q_{st}) (Jiang et al. 2003, 2004; Li et al. 2004). In this equation R is the universal gas constant, N_{ad} is the number of adsorbed molecules and U is the total energy of the system that consists of adsorbate–adsorbate and adsorbate–adsorbent both columbic and noncolumbic interactions. Introducing this relation is dependent on several approximations: adsorption reversibility and negligible molar volume of adsorbed gases, which have negligible effect on the survey of q_{st}. The calculated heats of adsorption are reported in Table 3.

Table 3 Isosteric heat of adsorption of slit models

	Slit-0	Slit-1	Slit-2	Slit-3
q_{st} (kJ/mol)	8.7999	9.8919	10.670	9.731

The order of isosteric heats of adsorption is: slit-0 < slit-3 < slit-1 < slit-2. So, the greater the loading of slit-2 with respect to the other slits at lower pressures can be explained by the magnitude of its isosteric heat of adsorption. The difference between the calculated q_{st} for slit-1 and 3 is small but the adsorption isotherms of slit-3 at all pressures are larger than that of the slit-1. Also, despite the greater heat of adsorption of slit-1 than slit-0, its adsorption amount is smaller than that of the slit-0. Both of these phenomena can be explained in terms of the narrow size of constricted region in slit-1, which is too small to accommodate a CH_4 molecule. So, the accessible volume in slit-1 is lower than the other slits and fewer adsorbate molecules can be adsorbed.

To elaborate details of the adsorption in the system, it was divided to slabs with 1 Å thickness in the y direction then the average densities of the adsorbed CH_4 molecules in each slab were calculated. The density profile of adsorbed CH_4 along the y axis is plotted in Fig. 4 for three selected pressures: 100, 500 and 1,000 kPa. The calculated adsorbate density is relatively equal for all slabs in slit-0 model, as expected.

The constricted slit model consists of two graphene sheets with two consecutive cusps to form the constricted region. For slit-1 at all pressures, no CH_4 molecule was adsorbed in the constricted region. However the two sharp peaks in the positions of two ends of constriction region and also two other peaks at the first cusps of the graphene sheets indicate the aggregation of adsorbate molecules in the position of two cusps of the graphene sheets. Figures 3 and 4 show that in this slit, the dominant adsorption occurs in the positions of the cusps. For slit-2 in the constricted region there is a wide peak with some downfalls in the constricted region… The two or three peaks can be attributed to the two or three adsorbed molecules in the constricted region. It must be mentioned here that the constricted region in slit-2 can only accommodate three methane molecules along the channel. In slit-3 a relatively broad peak appears in constricted region. It seems that the peak of constricted region is mixed up with the peak of the second cusp where it shows continuous adsorptive behavior near the constricted region. Figure 3 shows that the adsorbed molecules in the constricted region in slit 2 are aligned in one row in the middle of the channel but for slit 3 they are somewhat spread in the channel due to the larger diameter of the slit 3 relative to that of the slit 2. Two distant peaks are characterized by the methane adsorption by the carbon atoms of the graphene sheets in the first cusp.

It is interesting that in all three plots in Fig. 4, the densities in flat regions for each of the three slits are equal.

3.2 MD results

The radial distribution function can be used to explore the fluid microscopic structure around the pore walls. The radial distribution functions (RDF) have been obtained from the MD simulations (Allen and Tildesley 1987) of the equilibrated systems from the GCMC simulations. We have selected five carbon atoms of the pore wall in the vicinity of the constriction for which the RDF has calculated. Figure 5a shows the selected carbon atoms as C-1–5 located in the middle of the flat region, first and second

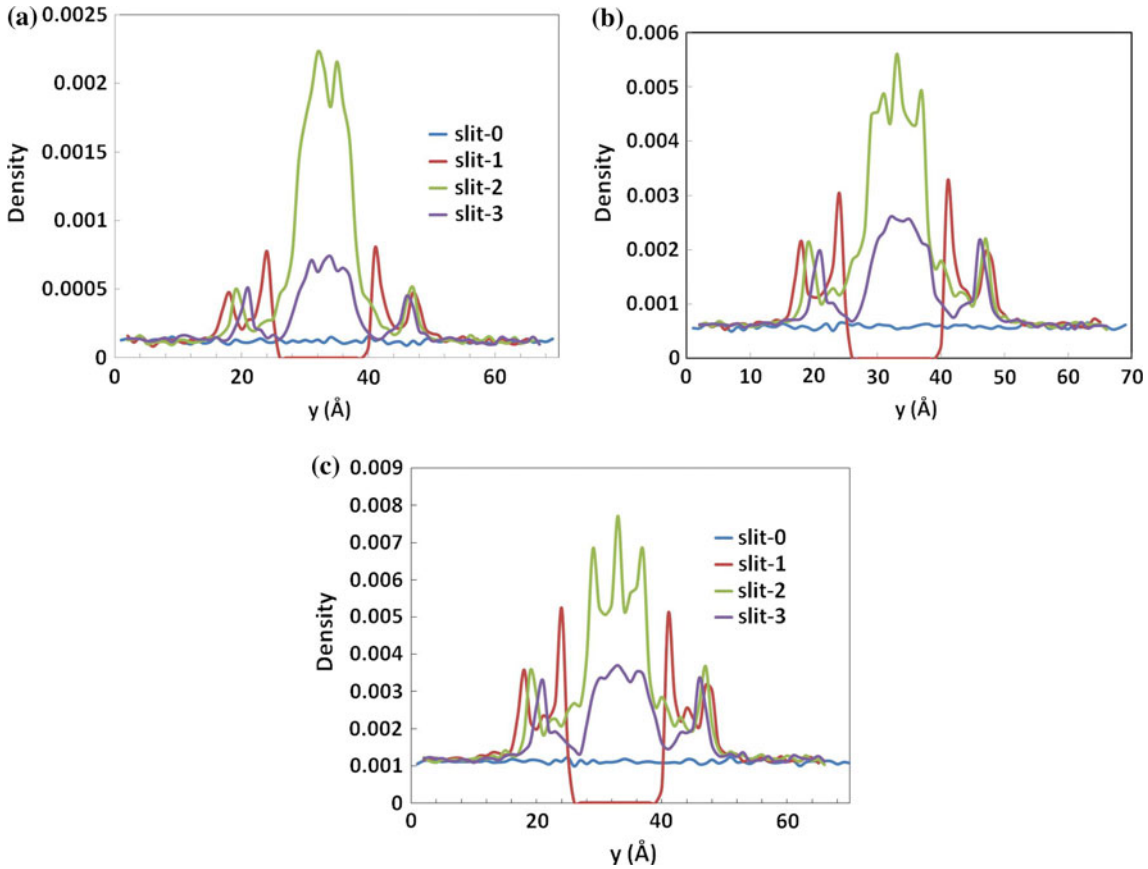

Fig. 4 Density profiles of adsorbed CH_4 in four studied models at pressures: **a** 100 kPa **b** 500 kPa and **c** 1,000 kPa

cusps of the graphene sheet, and in the middle of constriction regions, respectively.

Figure 5b–d show the calculated RDF of the carbon atom of methane and five specified carbon atoms in slit-2 at pressures 100, 500 and 1,000 kPa respectively. As shown in Fig. 5, at all three pressures the methane molecule was found within the 4 Å of C-5 and 6 Å of C-4; however the g(r) for the C-5 has a higher peak which indicates the larger adsorption at C-5. The height of the C-4 g(r) peak at 500 and 1,000 kPa increases which shows that the adsorbent reaches the saturation limit in the constriction region.

The calculated g(r) for C-1–3 shows well defined peaks at about 4.5 Å, but for C-3 the calculated g(r) presents one other broad peak at large distances. The calculated RDFs show that the methane molecules adsorbed mainly by the carbon atoms at the constricted region and carbon atoms at cusp positions of the graphene sheet.

Self-diffusion coefficient which generally describes the random motion of individual tagged particle in the absence of any gradient, was calculated for adsorbed methane molecules from the mean square displacement (MSD) of carbon atoms of methane using the Einstein relation (Arora and Sandler 2006; Dubbeldam and Snurr 2007; Mark and Nilsson 2001):

$$D_s(c) = \frac{1}{2dN} \lim_{t\to\infty} \frac{1}{t} \left\langle \sum_{i=1}^{N} [r_i(t) - r_i(0)]^2 \right\rangle \quad (2)$$

where $D_s(c)$ is the self-diffusion coefficient, N is the number of tagged particles in the system, d is the dimensionality of system, $r_i(t)$ is the position vector of particle i at time t and the brackets denote performing ensemble average.

In our studied system three directions are not equivalent for diffusing particle, so we calculated MSDs in three directions separately and then reported the calculated self-diffusion coefficients in x, y and z directions. The self-diffusion coefficients were estimated from the slope of the linear part of MSDs versus time at long times. The short time part of the correlation function is influenced by inertial effects and should not be included in the calculation (Mark and Nilsson 2001; Leroy 2004; Cao and Wu 2004). Table 4 represents the Self-diffusion coefficients of CH_4 in four slit models at four selected pressures 100, 500, 1000

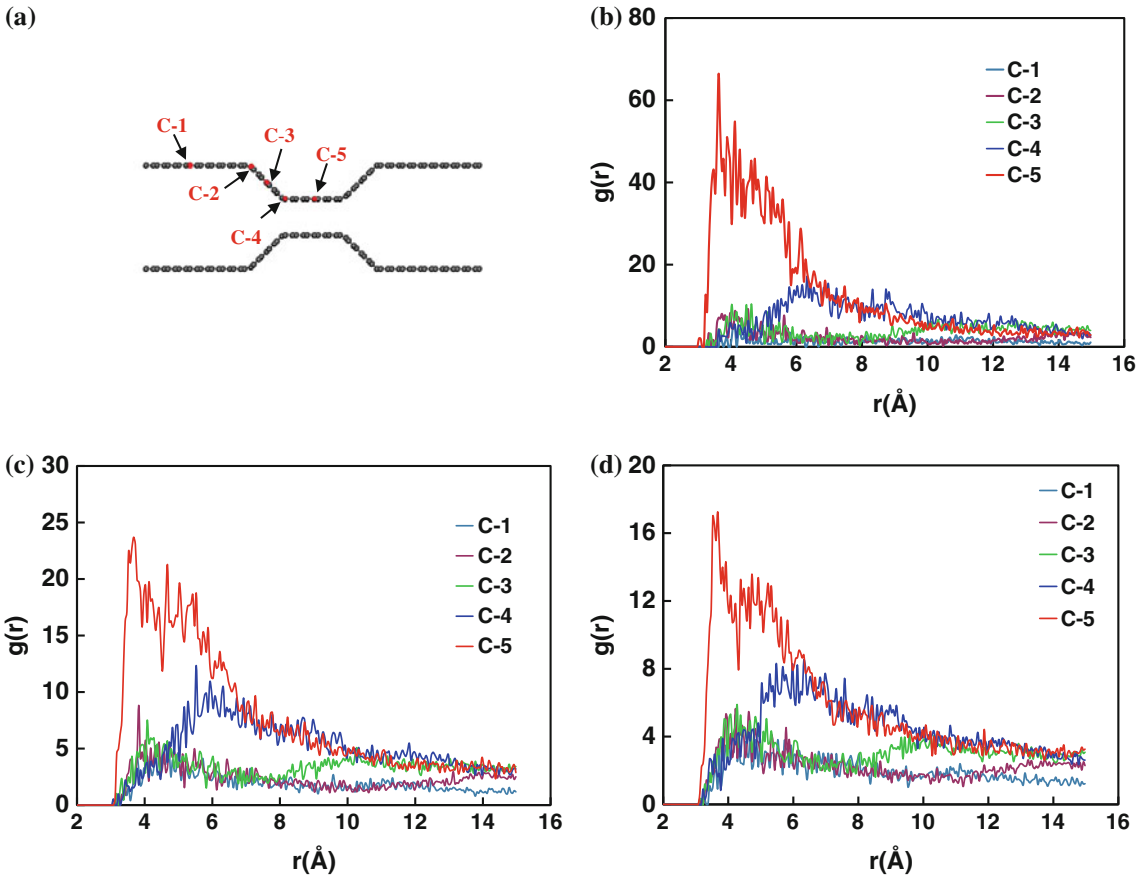

Fig. 5 **a** Selected carbon atoms of slit model. Radial distribution functions of dynamically equilibrated CH_4 molecules with respect to the specified carbon atoms of slit-2 at pressures of **b** 100 kPa, **c** 500 and **d** 1,000 kPa respectively

Table 4 Self diffusion coefficients (10^{-9} m^2/s) in 3 separated directions

Slit models	100 kPa			500 kPa			1,000 kPa			5,000 kPa		
	x	y	z	x	y	z	x	y	z	x	y	z
Slit-0	13.51	17.17	0.02	6.68	6.825	0.03	3.220	2.97	0.04	1.04	1.02	0.02
Slit-1	11.78	0.31	0.02	3.56	0.225	0.02	2.010	0.29	0.02	0.85	0.24	0.02
Slit-2	5.35	1.15	0.01	2.94	0.955	0.02	1.665	0.71	0.02	0.73	0.35	0.01
Slit-3	13.10	3.31	0.02	3.08	1.610	0.02	2.290	1.11	0.02	0.80	0.46	0.01

and 5,000 kPa which are calculated by averaging over the 1.0 ns trajectories. The pore width in the z direction is varying from 20 Å to the width of the constriction. As it can be seen from Table 4, the diffusion coefficient in this direction is much smaller than the other directions for all slits for four studied pressures. The low values of diffusion coefficient also have been observed in the y direction for slit-1. Regarding the structure of slit-1, as is shown in the snapshots, the constricted region is too narrow to allow the diffusion of methane molecules in the slit channel (y direction). The diffusion coefficients in the x and y directions for slits-2 and 3 are smaller than that of the slit-0, this difference is larger at a lower pressure in y direction. So, we can say that the constriction acts as a barrier of diffusion. The strong interaction in the constriction region prevents the rapid diffusion of particles. Particularly the slit-2 with the largest heat of adsorption, which results from stronger adsorption with two slit walls, has the lowest value of diffusion coefficients in x and y directions than slit-0 and 3. Also increasing the loaded molecules with pressure makes the diffusions to be lower.

Because of the dependency of experimental diffusivity values to instrumental techniques and their related theories, and the scarce works which report methane diffusion coefficients in carbon materials, it is difficult to compare the self-diffusivities obtained in this work with the experimental values (Ramı′rez 2011). In spite of this, the self-diffusion coefficient of methane obtained in this study in y direction of the slit-2 can be compared to experimental effective self-diffusivities for methane in carbon molecular sieve (CMS) membranes. Yoshimune et al. (2007) were obtained the diffusion coefficient of methane in CMS as of 0.25×10^{-12} m^2/s at $T = 298$ K and $P = 1$ bar. Whereas Lim and Bhatia (2011) were reported the values ranging from 5.0×10^{-9} to 17.5×10^{-9} m^2/s at temperatures ranging from 298 to 318 K and pressures from about 0.01 to 100 bar. Their results are about 2.0×10^4 to 7.0×10^4 times larger than the experimental value. Our calculated diffusion coefficient of methane in the slit-2 in the same condition as Yoshimune's study is 1.155×10^{-9} m^2/s, that though is about 4.62×10^3 times greater than Yoshimune's experimental result but is 4.3–15.15 times lower than Lim's result. Although our results show that the constricted slit model is superior to the flat slit in predicting the diffusion behavior of the methane in NPCs but it is far from providing a satisfactory description of molecular diffusion in NPCs. The work on the improvement of the constricted slit model is going on in our lab.

4 Conclusions

We used GCMC and MD simulations for studying adsorption and dynamic behavior of methane in the interior of constricted slit models: slit-1, 2 and 3 with constriction heights: 5, 7 and 9 Å. For comparison we also used the traditional flat slit titled with slit-0. We have used an all atom model for methane molecules. The adsorption isotherms that achieved from the GCMC simulation show that introducing the constriction generally increases the adsorbed amount despite of its width. The slit-2 with the constriction height of 7 Å has the highest uptake of methane at pressures up to 3,000 kPa and the greatest isosteric heat of adsorption. For this slit one layer of methane molecules can be fitted in the constricted part of the slit. The snapshots and the density profiles of the equilibrated system reveals that in slit-2 one layer adsorption has occurred, whereas in slit-1 no CH_4 molecule can be placed in the constriction and for slit-3 with wider constriction more than one layer was adsorbed. These results show that at low pressures methane will be adsorbed more by the constricted slits with a constriction width close to the molecular diameter.

The RDFs of methane and five specified carbon atoms in slit-2 have shown that the methane molecules adsorb mainly by the carbon atoms at the constricted region and carbon atoms at cusp positions of the graphene sheet. Using the MSD plots that obtained from MD simulations, we calculated the self-diffusion coefficient of CH_4 molecules within four studied slit models at 100, 500, 1000 and 5,000 kPa of pressures. It is found in all studied cases, the calculated diffusion coefficients for constricted slits are lower than the

flat slit. The constricted slit models represent better dynamic results rather than flat slit by introducing the relatively lower diffusion amounts.

Acknowledgments We thank the financial support of this work by university of Mazandaran.

References

Ahmad, F., Mukhtar, H., Man, Z., Dutta, B.K.: A theoretical analysis of non-chemical separation of hydrogen sulfide from methane by nano-porous membranes using capillary condensation Chem. Eng. Process **47**(12), 2203–2208 (2008)

Allen, M.P., Tildesley, D.J.: Computer Simulation of Liquids, pp. 110–135. Oxford University Press, New York (1987)

Anderson, C.J., Tao, W., Jiang, J., Sandler, S.I., Stevens, G.W., Kentish, S.E.: An experimental evaluation and molecular simulation of high temperature gas adsorption on nanoporous carbon. Carbon **49**, 117–125 (2011)

Arora, G., Sandler, S.I.: Nanoporous carbon membranes for separation of nitrogen and oxygen: insight from molecular simulations. Fluid Phase Equilib. **259**, 3–8 (2007)

Arora, G., Sandler, S.I.: Mass transport of O_2 and N_2 in nanoporous carbon (C_{168} Schwarzite) using a quantum mechanical force field and molecular dynamics simulations. Langmuir **22**, 4620–4628 (2006)

Billemont, P., Coasne, B., Weireld, G.D.: An experimental and molecular simulation study of the adsorption of carbon dioxide and methane in nanoporous carbons in the presence of water. Langmuir **27**(3), 1015–1024 (2011)

Cao, D., Wu, J.: Self-diffusion of methane in single-walled carbon nanotubes at sub- and supercritical conditions. Langmuir **20**, 3759–3765 (2004)

Coasne, B., Gubbins, K. E., Hung, F.R., Jain, S. K.: Adsorption and structure of argon in activated porous Carbons. Mol. Sim. **32**(7), 557–566 (2006a)

Coasne, B., Jain, S. K., Gubbins, K. E.: Adsorption, structure and dynamics of fluids in ordered and disordered models of porous carbons. Mol. Phys. **104**, 3491–3499 (2006b)

Coasne, B., Alba-Simionesco, Ch., Audonnet, F., Dosseh, G., Gubbins, K. E.: Adsorption, structure and dynamics of benzene in ordered and disordered porous carbons. Phys. Chem. Chem. Phys. **13**, 3748–3757 (2011)

Dubbeldam, D., Snurr, R.Q.: Recent developments in the molecular modeling of diffusion in nanoporous materials. Mol. Sim. **33**(4), 305–325 (2007)

Esteves, I.A.A.C., Lopes, M.S.S., Nunes, P.M.C., Mota, J.P.B.: Adsorption of natural gas and biogas components on activated carbon. Sep. Purif. Technol. **62**, 281–296 (2008)

Fan, C., Do, D.D., Nicholson, D.: On the cavitation and pore blocking in slit-shaped ink-bottle pores. Langmuir **27**, 3511–3526 (2011)

Firouzi, M., Wilcox, J.: Molecular modeling of carbon dioxide transport and storage in porous carbon-based materials. Microporous Mesoporous Mater. **158**, 195–203 (2012)

Foroutan, M., Nasrabadi, A.T.: Adsorption and separation of binary mixtures of noble gases on single-walled carbon nanotube bundles. Physica E **43**, 851–856 (2011)

Golebiowska, M., Roth, M., Firlej, L., Kuchta, B., Wexler, C.: The reversibility of the adsorption of methane-methyl mercaptan mixtures in nanoporous carbon. Carbon **50**, 225–234 (2012)

Heuchel, M., Davies, G.M., Buss, E., Seaton, N.A.: Adsorption of carbon dioxide and methane and their mixtures on an activated carbon: simulation and experiment. Langmuir **15**, 8695–8705 (1999)

Ho, T.A., Argyris, D., Cole, D.R., Striolo, A.: Aqueous NaCl and CsCl solutions confined in crystalline slit-shaped silica nanopores of varying degree of protonation. Langmuir **28**, 1256–1266 (2012)

Jagiello, J., Olivier, J.P.: A simple two-dimensional NLDFT model of gas adsorption in finite carbon pores. Application to pore structure analysis. J. Phys. Chem. C **113**, 19382–19385 (2009)

Jiang, J., Klauda, J.B., Sandler, S.I.: Monte Carlo simulation of O_2 and N_2 adsorption in nanoporous carbon (C_{168} schwarzite). Langmuir **19**, 3512–3518 (2003)

Jiang, J., Klauda, J.B., Sandler, S.I.: Hierarchical modeling O_2 and N_2 adsorption in C_{168} Schwarzite: from quantum mechanics to molecular simulation. J. Phys. Chem. B **108**, 9852–9860 (2004)

Leroy, F., Rousseau, B., Fuchs, A.H.: Self-diffusion of *n*-alkanes in silicalite using molecular dynamics simulation: a comparison between rigid and flexible frameworks. Phys. Chem. Chem. Phys. **6**, 775–783 (2004)

Li, Sh, Falconer, J.L., Noble, R.D.: SAPO-34 membranes for CO_2/CH_4 separation. J. Membr. Sci. **241**, 121–135 (2004)

Lim, Y., Bhatia, S.K.: Simulation of methane permeability in carbon slit pores. J. Membr. Sci. **369**, 319–328 (2011)

López, M.J., Cabria, I., Alonso, J.A.: Simulated porosity and electronic structure of nanoporous carbons. J. Chem. Phys. **135**, 104706–104709 (2011)

Lucenaa, S.M.P., Frutuosoa, L.F.A., Silvino, P.F.G., Azevedoa, D.C.S., Tosob, J.P., Zgrablichb, G., Cavalcante Jr, C.L.: Molecular simulation of collection of methane isotherms in carbon material using all-atom and united atom models. Colloid Surf. **A357**, 53–60 (2010)

Mark, P., Nilsson, L.: Structure and dynamics of the TIP3P, SPC, and SPC/E water models at 298 K. J. Phys. Chem. A **105**, 9954–9960 (2001)

Nasrabadi, A.T., Foroutan, M.: Air adsorption and separation on carbon nanotube bundles from molecular dynamics simulations. Compute Mater. Sci. **61**, 134–139 (2012)

Nguyen, P.T., Do, D.D., Nicholson, D.: On the cavitation and pore blocking in cylindrical pores with simple connectivity. J. Phys. Chem. B **115**, 12160–12172 (2011)

Palmer, J.C., Moore, J.D., Brennan, J.K., Gubbins, K.E.: Adsorption and diffusion of argon in disordered nanoporous carbons. Adsorption **17**, 189–199 (2011)

Palmer, J.C., Gubbins, K.E.: Atomistic models for disordered nanoporous carbons using reactive force fields. Microporous Mesoporous Mater. **154**, 24–37 (2012)

Peng, L., Morris, J.R.: Prediction of hydrogen adsorption properties in expanded graphite model and in nanoporous carbon. J. Phys. Chem. C **114**, 15522–15529 (2010)

Ramı′rez, A.: A kinetic Monte Carlo approach to diffusion in disordered nanoporous carbons. Chem. Eng. Sci. **66**, 5663–5671 (2011)

Severson, B.L., Snurr, R.Q.R.Q.: Monte Carlo simulation of n-alkane adsorption isotherms in carbon slit pores. J. Chem. Phys. **126**, 134708 (2007)

Sitprasert, C., Zhu, Z.H., Wang, F.Y., Rudolph, V.: A multi-scale approach to the physical adsorption in slit pores. Chem. Eng. Sci. **66**, 5447–5458 (2011)

Smith, W., Forester, T.R., Todorov, I.T.: STFC Daresbury Laboratory, Version 2.20, Daresbury, Warrington, (2009)

Striolo, A., Chialvo, A.A., Cummings, P.T., Gubbins, K.E.: Water adsorption in carbon-slit nanopores. Langmuir **19**, 8583–8591 (2003)

Wang, W., Peng, X., Cao, D.: Capture of trace sulfur gases from binary mixtures by single-walled carbon nanotube arrays: a molecular simulation study. Environ. Sci. Technol. **45**, 4832–4838 (2011)

Yoshimune, M., Fujiwara, I., Haraya, K.: Carbon molecular sieve membranes derived from trimethylsilyl substituted poly(phenylene oxide) for gas separation. Carbon **45**, 553–560 (2007)